GEOPHYSICAL RESEARCH LETTERS, VOL. 25, NO. 8, PAGES 1229-1232, APRIL 15, 1998

Seismic anisotropy in the lowermost mantle beneath the Pacific

Jeroen Ritsema,[1] Thorne Lay,[2] Edward J. Garnero,[3] and Harley Benz[4]

Abstract. Onset time differences of up to 3 s are observed between transverse (S^{SH}) and longitudinal (S^{SV}) components of broadband S waves at distances of 85° to 120° for paths traversing the lowermost mantle (D") beneath the Pacific. After correction for upper mantle anisotropy, S^{SH} usually arrives earlier than S^{SV} with the splitting increasing with distance from 100° to 120°. The data yield two possible models of anisotropy: (1) anisotropy may vary laterally, with transverse isotropy existing in higher–than–average shear velocity regions beneath the northeastern Pacific, or (2) anisotropy may vary with depth, with transverse isotropy concentrated in a thin (100 km) thermal boundary layer at the base of D". A few recordings at distances less than 105° show that S^{SV} arrives earlier than S^{SH}, indicating that general anisotropy likely exists in shallower regions of D".

1. Introduction

Flow dynamics, small-scale layering, and mineralogy in the lowermost 200–300 km of the mantle (D") can potentially be constrained by observations of seismic anisotropy [e.g., *Lay et al.*, 1998]. Seismic anisotropy in D" is primarily analyzed using ScS, S and $S_{\rm diff}$ shear wave recordings at distances larger than 70°. When anisotropy is apparent, the transverse (S^{SH} or ScS^{SH}) component usually arrives earlier than the longitudinal (S^{SV} or ScS^{SV}) component of shear motion [e.g., *Lay and Young*, 1991; *Kendall and Silver*, 1996; *Matzel et al.*, 1996; *Garnero and Lay*, 1997]. This is consistent with the presence of transverse isotropy (TI) with a vertical symmetry axis, which may result from thin horizontal lamellae with strong velocity contrasts [*Backus*, 1962].

However, lateral variation of the symmetry and magnitude of seismic anisotropy in D" is also evident. *Pulliam and Sen* [1997] report observations of S^{SV} preceding S^{SH} in S wave recordings of Tonga-Fiji earthquakes at station HKT (Hockley, Texas), while recordings at more distant stations in the northeastern United States indicate a transition to TI [e.g., *Vinnik et al.*, 1995]. We further explore the spatial variations of seismic anisotropy beneath the Pacific using an extensive data set of S and $S_{\rm diff}$ wave recordings from broadband stations in North America.

2. Measurement of Seismic Anisotropy

Anisotropy in D" produces subtle effects on S waveforms [*Maupin*, 1994], These effects are not easily modeled because the presence of radial velocity gradients in D" and the strong velocity contrast at the core-mantle boundary (CMB) result in non-linear S and $S_{\rm diff}$ polarizations that are model dependent. This is illustrated in Figure 1 for shear velocity models PREM [*Dziewonski*

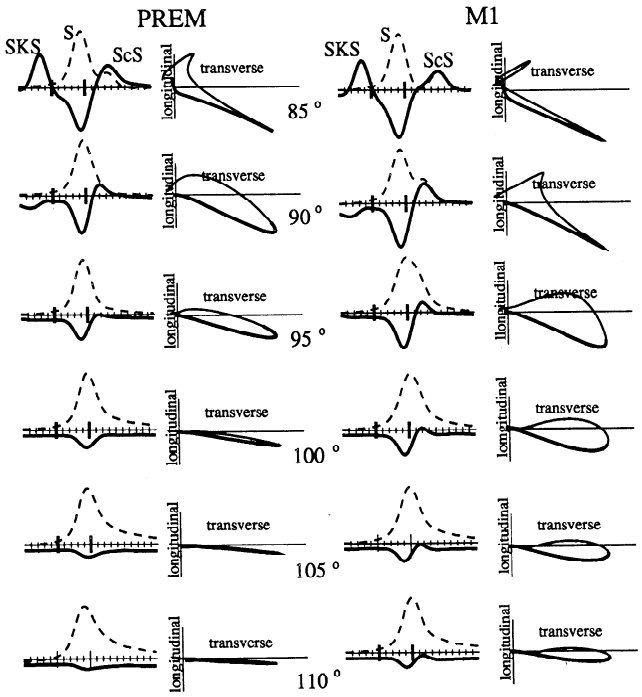

Figure 1. Synthetic waveforms of longitudinal (solid lines) and transverse (dashed lines) component shear waves at distances between 85° and 110° for models PREM and M1. The waveforms have a duration of 30 s and have been normalized by the maximum amplitude of the transverse component. Particle motions are shown to the right of the waveforms. The particle motion represented by the heavy thick line is for the 10 s interval indicated by the bold ticks on the waveforms.

[1]Department of Geological Sciences, University of South Carolina, Columbia. Now at Seismological Laboratory, California Institute of Technology, Pasadena

[2]Institute of Tectonics, University of California, Santa Cruz

[3]Berkeley Seismological Laboratory, University of California, Berkeley

[4]United States Geological Survey, Boulder

Paper number 98GL00913.
0094-8534/98/98GL-00913$05.00

Table 1. Earthquake Source Coordinates

Date	Lat. (°S)	Lon. (°W)	Depth (km)
June 8, 1990	18.7	181.1	499
June 26, 1990	22.0	180.5	593
July 22, 1990	23.5	180.1	565
Sep. 30, 1991	21.0	181.4	580
Dec. 3, 1991	26.3	178.6	581
July 11, 1992	22.3	181.5	381
Aug. 30, 1992	17.7	181.2	573
March 21, 1993	18.0	181.5	584
Aug. 7, 1993	23.9	179.8	555
March 9, 1994	17.8	181.5	564
March 31, 1994	22.0	180.4	591
Jan. 17, 1995	20.9	180.8	637
Aug. 5, 1996	20.8	181.9	535
Oct. 19, 1996	20.4	181.6	604
Nov. 5, 1996	31.1	180.3	369
March 21, 1997	31.1	179.9	450

and Anderson, 1981], which has a mild positive gradient in D", and M1 [*Ritsema et al.*, 1997], which has a strong negative gradient in the lowermost 200 km of the mantle, as is appropriate for the average D" structure beneath the Pacific. Non-linear S wave polarization, obvious in even the first half cycle of the S wave, is caused by interference of ScS, SKS and $SKKS$, and by diffraction along the CMB. The interference effects on the transverse and longitudinal components are different for PREM and M1.

We infer the presence of anisotropy from the difference in the arrival times of S^{SV} and S^{SH}. We use onset times of S^{SH} and S^{SV} which are, in contrast to waveshapes, not affected by variations in isotropic structure. Absence of onset time differences does not preclude the existence of general anisotropy, but the anisotropy must then be constrained by waveform modeling. We denote the differential arrival time of S^{SV} and S^{SH} as T_{SV-SH}. The magnitude of anisotropy, χ (in percent), is defined as $100 \times [1 - \frac{V_{SV}}{V_{SH}}]$, where V_{SV} and V_{SH} represent 'apparent' shear velocities of S^{SV} and S^{SH} consistent with T_{SV-SH} for a prescribed path length.

After analysis of 163 recordings from 16 deep Tonga-Fiji earthquakes (Table 1), we retain 84 broadband S and S_{diff} recordings, which yield impulsive S^{SV} and S^{SH} onsets for phases that are well isolated from the core phases SKS and $SKKS$ and that are well above the amplitude level of seismic coda. T_{SV-SH} for these data can be measured within a 1-s accuracy. Both S^{SH} and S^{SV} propagate efficiently through D" beneath the Pacific because of a negative shear velocity gradient in the lowermost mantle [*Ritsema et al.*, 1997]. Therefore, recordings at epicentral distances between 85° and 120° can be utilized.

The broadband signals are deconvolved by the instrument response to obtain displacement ground motions. A low pass filter with a corner period of 5 s is applied. We account for upper mantle anisotropy following *Garnero and Lay* [1997], using SKS-derived 'splitting parameters' that have been determined for nearly all digital broadband stations in North America [e.g., *Silver*, 1996]. We emphasize the larger anomalies (2–3 s) in our measurements as these are unlikely to be associated with unrecognized receiver effects or inaccurately picked onset times. Application of the receiver corrections does not systematically reduce the splitting measurements, and leaves the spatial patterns unchanged.

3. Observations of Seismic Anisotropy

Thirteen positive and four negative values of T_{SV-SH} larger than our 1-s noise level are found. The overall data set shows a distance dependence (Figure 2) that will be considered below. Six sets of S waveforms and particle motions with T_{SV-SH} values ranging from +1.8 to +3.6 s (S^{SH} preceding S^{SV}) are shown in Figure 3. Anisotropy is manifested in the clear delays of the S^{SV} onsets with respect to the S^{SH} onsets and in the purely transverse particle motions that immediately follow the S^{SH} onsets. The particle motions of three of the five large-distance recordings have clockwise orientations in contrast to predictions for the M1 shear velocity structure (see Figure 1). This feature is consistent with a delay of S^{SV} with respect to S^{SH}. Additional HRV (Harvard, Massachusetts) recordings indicating TI have been shown by *Vinnik et al.* [1995].

Waveforms with negative values of T_{SV-SH} (S^{SV} preceding S^{SH}) are shown in Figure 4. These recordings show early onsets of S^{SV} and purely longitudinal polarizations immediately follow the onsets. Similar observations are presented by *Pulliam and Sen* [1997].

4. Spatial Patterns of D" Anisotropy

The observations of T_{SV-SH} have the spatial characteristics shown in Figure 5. Figure 5a shows the lateral distribution of paths with different splitting values. Paths associated with large, positive values of T_{SV-SH} extend to D" regions with higher-than-average shear velocity structure [*Grand et al.*, 1997], while S paths associated with negative or 'near-zero' values of T_{SV-SH} are within, or near low shear velocity regions of D".

Assuming that the large positive T_{SV-SH} observations accrue while S propagates through higher-than-

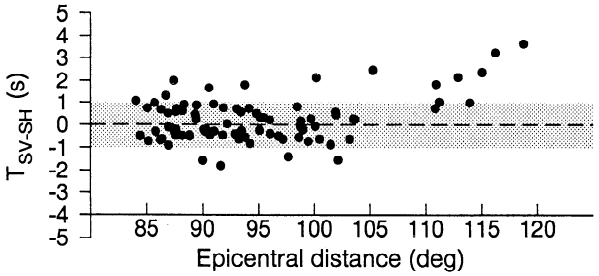

Figure 2. Distance dependence of T_{SV-SH}. Values of T_{SV-SH} included in the grey shaded region are considered to be statistically insignificant.

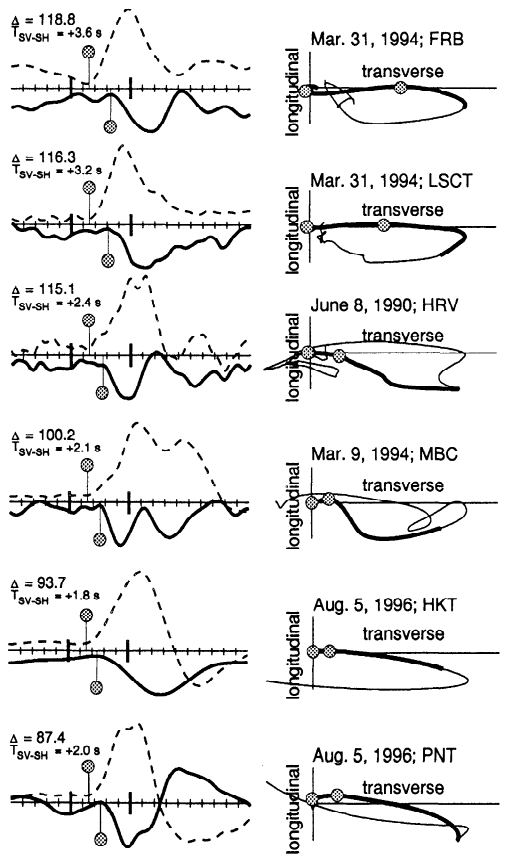

Figure 3. Longitudinal (solid line) and transverse (dashed lines) component S waveforms showing S^{SH} signals that arrive earlier than S^{SV}. The recordings are scaled such that the maximum amplitude of S^{SH} is two times larger than the maximum S^{SV} amplitude. The epicentral distance (Δ) and T_{SV-SH} (denoted as Δt) are plotted at the upper left of the waveforms. Onset times are marked by vertical lines with grey shaded circles. Particle motions are plotted to the right of the waveforms with grey circles corresponding to the onset times. Ten seconds of particle motion are represented by heavy lines for a time interval indicated by heavy tick marks in the waveform plots.

average shear velocity structure in a 300 km thick D" layer, we estimate path lengths of about 1000 km using the M1 shear velocity model. Values of T_{SV-SH} between 2 s and 3 s yield an estimate of χ of about 1.4% to 2.1%, with the uncertainty arising from the assumptions of D" thickness and the velocity model used to estimate the propagation length (using PREM increases the predicted path lengths in D" and thus reduces the estimate of the magnitude of anisotropy by 20–50%).

Figure 5b presents an alternate possibility: the high T_{SV-SH} values at the largest epicentral distances (Figure 2) suggest that TI is concentrated within a thin layer just above the CMB, as the largest splitting values are generally associated with the deepest penetrating rays. Model M1 was used to compute the turning points in D" for each path. For model PREM the pattern is similar, although raypaths are somewhat closer to the CMB. Assuming that T_{SV-SH} is caused by TI in the lowermost 100 km of the mantle, we estimate an average value of χ of about 1.5%. The TI region need not vary laterally, but it must be overlain by a zone of variable general anisotropy.

5. Discussion and Conclusions

Kendall and Silver [1996] explain the co-existence of high shear velocity and TI structure beneath the Caribbean by partial melting of former-basaltic layers within subducted oceanic slab that has penetrated to D" and flattened out above the CMB. For the Pacific, the regions with TI are only modestly high shear velocity, and are not obviously related to regions of subducted slab. The strong TI found beneath Alaska [e.g., *Lay and Young*, 1991; *Matzel et al.*, 1996; *Garnero and Lay*, 1997] may extend to our more northerly anomalies, but a very broad area would then appear to have TI.

The possibility that TI is concentrated in the lowermost 100 km of the mantle is intriguing. This is about the scale length for the expected thermal boundary layer above the CMB. This region should have a strongly increasing temperature and a rapidly decreasing viscosity with increasing depth. Large TI effects may be induced by strong horizontal flows in the boundary layer, possibly associated with thermal upwellings in the southwestern portion of our study area. The intermittent observations of both positive and negative values of T_{SV-SH} for paths in the southwestern region indicate the presence of general anisotropy that is not aligned favorably with respect to the great-circle paths. General anisotropy is expected in a regime with com-

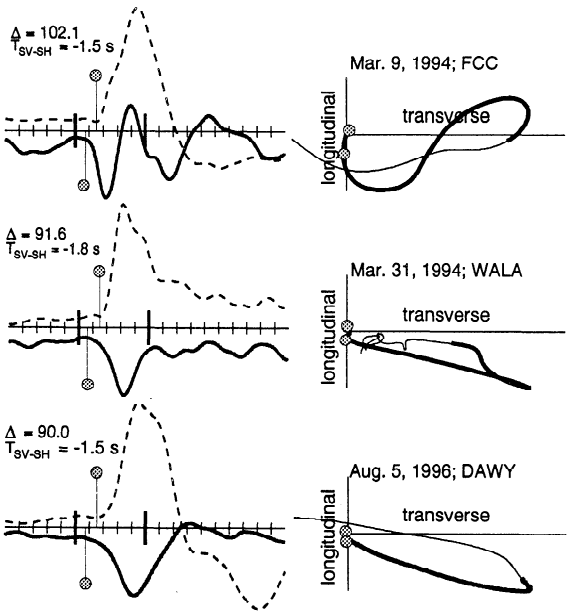

Figure 4. S waveforms with S^{SV} arrivals preceding S^{SH}. See Figure 4 for details.

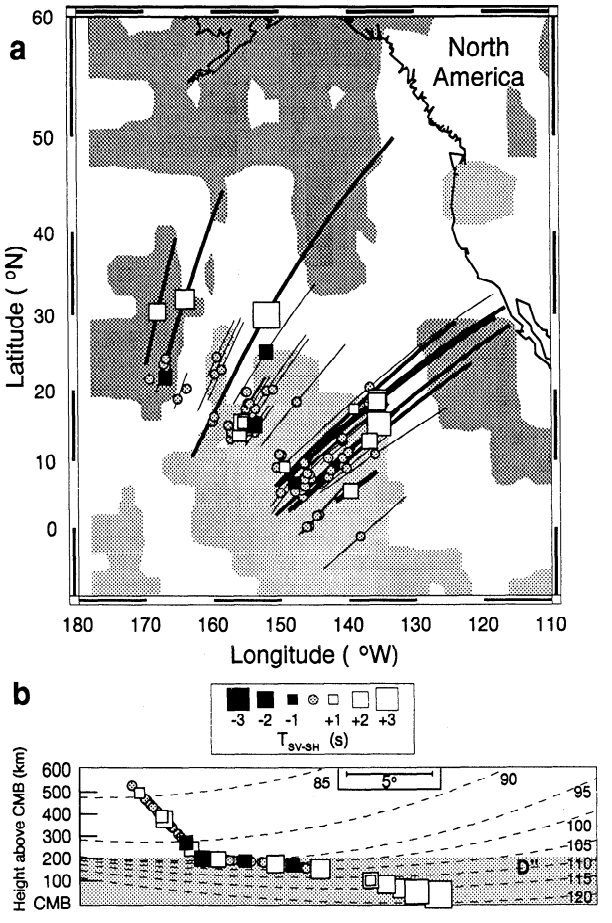

Figure 5. (a) Lateral distribution of T_{SV-SH} for paths beneath the Pacific. White squares represent T_{SV-SH} measurement greater than 1 s and black squares represent T_{SV-SH} values less than -1 s. These symbols are plotted at S turning points in D". The size of the symbol is proportional to the magnitude of T_{SV-SH} (χ). Data points represented by grey circles have absolute T_{SV-SH} values smaller than 1 s. The black lines are surface projections of S paths through the lowermost 200 km of the mantle. Thick black lines are paths associated with T_{SV-SH} times larger than +1 s. The grey shades are the high (> 0.5%) (dark) and low (< -0.5%) (light) shear velocity regions in the lowermost mantle layer (2650–2890 km depth) of the model by *Grand et al.* [1997]. (b) Locations of S wave turning points (computed using model M1) in a cross-section through the lower mantle, assuming a common source location and receiver azimuth for all data. Dashed lines are S paths between 85° and 120°. The symbols are the same as in the map.

plex, but predominantly vertical flow (see also *Pulliam and Sen*, [1997]).

The ultra low velocity layer of partial melt at the base of the mantle [e.g., *Williams and Garnero*, 1996] may play an important role in developing TI structures in the thermal boundary layer above the CMB. Partial melting should accentuate viscosity reductions, horizontal shear flows, and mixing of chemical heterogeneities that may result in anisotropy.

Acknowledgments. Data were provided by the Data Management Center of IRIS. All figures were generated with the GMT software of *Wessel and Smith* [1991]. We thank the anonymous reviewers for their comments. This research is funded under NSF grants EAR-9706663, EAR-9418643, and EAR-9305894. Contribution number 344 of the Institute of Tectonics, UCSC.

References

Backus, G. E., Long-wave elastic anisotropy produced by horizontal layering, *J. Geophys. Res.*, *67*, 4427–4440, 1962.

Dziewonski, A. M., and D. L. Anderson, Preliminary reference Earth model, *Phys. Earth Plan. Inter.*, *25*, 297–356, 1981.

Garnero, E. J., and T. Lay, Lateral variations in lowermost mantle shear wave anisotropy beneath the north Pacific and Alaska, *J. Geophys. Res.*, *102*, 8121–8135, 1997.

Grand, S. P., R. D. Van der Hilst, and S. Widiyantoro, Global seismic tomography: A snap shot of convection in the Earth, *GSA Today*, *7*, 1–7, 1997.

Kendall, J.-M., and P. G. Silver, Constraints from seismic anisotropy on the nature of the lowermost mantle, *Nature*, *381*, 409–412, 1996.

Lay, T., and C. J. Young, Analysis of seismic SV waves in the core's penumbra, *Geophys. Res. Lett.*, *18*, 1373–1376, 1991.

Lay, T., E. J. Garnero, Q. Williams, L. Kellogg, and M. E. Wysession, Seismic wave anisotropy in the D" region and its implications, in The Core-Mantle Boundary, eds. M. Gurnis, E. Knittle, M. Wysession, and B. A. Buffett, American Geophysical Union, in press, 1998.

Matzel, E., M. K. Sen, and S. P. Grand, Evidence for anisotropy in the deep mantle beneath Alaska, *Geophys. Res. Lett.*, *23*, 2417–2420, 1996.

Maupin, V., On the possibility of anisotropy in the D" layer as inferred from the polarization of diffracted S waves, *Phys. Earth Planet. Inter.*, *87*, 1–32, 1994.

Pulliam, J., and M. K. Sen, Anisotropy in the core-mantle transition zone may indicate chemical heterogeneity, *Geophys. J, Int.*, in review, 1997.

Ritsema, J., E. Garnero, and T. Lay, A strongly negative shear velocity gradient and lateral variability in the lowermost mantle beneath the Pacific, *J. Geophys. Res.*, *102*, 20,395–20,411, 1997.

Silver, P. G., Seismic anisotropy beneath the continents: Probing the depths of geology, *Annu. Rev. Earth Planet. Sci.*, *24*, 385–432, 1996.

Vinnik, L., B. Romanowicz, Y. LeStunff, and L. Makeyeva, Seismic anisotropy in the D" layer, *Geophys. Res. Lett.*, *22*, 1657–1660, 1995.

Wessel, P., and W. H. F. Smith, Free software helps map and display data, *Eos Trans. AGU*, *72*, 441, 445–446, 1991.

Williams Q., and E. J. Garnero, Seismic evidence for partial melt at the base of Earth's mantle, *Science*, *273*, 1528–1530, 1996.

H. Benz, United States Geological Survey, Boulder, CO 80225. (e-mail: benz@gldage.cr.usgs.gov)

E. J. Garnero, Berkeley Seismological Laboratory, University of California, Berkeley, CA 94720. (e-mail: eddie@seismo.berkeley.edu)

T. Lay, Institute of Tectonics, University of California, Santa Cruz, CA 95064. (e-mail: thorne@earthsci.ucsc.edu)

J. Ritsema, Seismological Laboratory, California Institute of Technology, Pasadena, CA 91125. (e-mail: jeroen@gps.caltech.edu)

(Received November 20, 1997; revised March 2, 1998; accepted March 6, 1998.)